Experimental Studies of Shock Wave-Related Phenomena at the Ben-Gurion University: A Review

O. Sadot

Abstract The shock tube laboratory at the Ben-Gurion University was founded at the early 1970s by Profs. Ozer Igra and Gabi Ben-Dor. About two decades later, the system was reassembled and altered to investigate the Richtmyer-Meshkov instability (RMI). Recruiting new students (including myself) and a well-known scientist, Dr. Alex Britan RIP, the research activities expanded and became deeper. New shock tubes were constructed, new diagnostic techniques were implemented, and new equipment were purchased. In the presentation, some studies that were conducted during the past two decades and not published yet in the open literature will be presented. One of the main objectives of the study in the laboratory has been the RMI. In this study, a shock wave crosses the interface between two fluids having different densities and accelerates it. As a result, the interface becomes unstable and small perturbations grow nonlinearly. We were interested in the evolution of a well-defined multimode initial perturbation. Another subject that was intensely investigated was the starting process in a nozzle. We investigated the problem with two aims: (a) to better understand the effect of asymmetry of the nozzle on the flow inside it and (b) to better understand the flow in the nozzle when different pressure profiles initiated the flow.

1 General Introduction

The shock tube laboratory at the Ben-Gurion University was founded at the early 1970s by Profs. Ozer Igra and Gabi Ben-Dor. The aim of the system was to investigate shock wave-related phenomena. The explosive-driven driver section

This paper was invited by the conference organizers.

O. Sadot (✉)
Department of Mechanical Engineering, Faculty of Engineering Sciences, Ben-Gurion University of the Negev, Beer Sheva, Israel
e-mail: sorens@bgu.ac.il

A. Sasoh et al. (eds.), *31st International Symposium on Shock Waves 1*,
https://doi.org/10.1007/978-3-319-91020-8_4

was the barrel of a 122 lb Canadian canon. The driver that operated only once didn't reach the expected requirements. About two decades later, the system was reassembled and altered to investigate the Richtmyer-Meshkov (RM) instability. Recruiting new students (including myself) and a well-known scientist, Dr. Alex Britan RIP, the research activities expanded and became deeper. New shock tubes were constructed, new diagnostic techniques were implemented, and new equipment were purchased.

In the paper and presentation, I will focus on two studies that were conducted during the past decade that have not been published yet in the open literature:

(a) The RM instability under re-shock conditions. This study was conducted by my PhD student A. Formoza.
(b) The starting process in a converging-diverging nozzle. This study was conducted by my two MSc students R. Zeltser and Y. Shahak.

These two subjects have little in common; therefore the paper like the presentation is split into these two subjects. First, the RMI study will be presented.

2 Richtmyer-Meshkov Instability

2.1 Introduction

The Rayleigh-Taylor (RT) [1, 2] and the Richtmyer-Meshkov (RM) [3, 4] instabilities are subject of intensive experimental and theoretical research due to their crucial importance in inertial confinement fusion (ICF) [5] and their major role in understanding astrophysical phenomena such as core-collapse supernovae [6]. The RM instability is developed at the contact surface between two fluids having different densities, which are accelerated impulsively. In a shock tube, this is achieved by means of a shock wave that crosses the interface. In contrast to the RT instability, the RM instability is developed in both cases where the acceleration is either from the light fluid to the heavy one or from the heavy fluid to the light one. In order to describe the instability evolution, two different approaches were introduced: the real space [7] and the Furrier space [8] approaches. Both approaches predict a linear growth in the early stages of the instability evolution followed by a nonlinear stage in which bubble competition or mode coupling play major roles. In the real space picture, Layzer [9] introduced a model for the RT instability that was expanded later by Hecht et al. [10] to include the RM instability. The model described the evolution of a single bubble (a chunk of light fluid penetrating into the heavy fluid layer) or two neighboring bubbles having different initial shapes. These models showed that the RM single-bubble velocity initially grows linearly as predicted by Richtmyer [3] while reducing its velocity as time progresses. The velocity decreases from its linear velocity to the asymptotic form as:

$$v_{\text{asy}} \propto \frac{\lambda}{t} \tag{1}$$

where λ is the wavelength of the bubble and t is time. In the case of a multi-bubble configuration, after the linear stage, the bubble velocity is affected by the neighbor bubbles. In this case the geometry of the interface surrounding the bubble plays a major role. Two different approaches were taken in order to describe the nonlinear interface behavior: the Furrier space and the real space approaches. In the Furrier space approach, the interface is constructed from modes, while as time progresses there is a migration of short wavelength modes to lower modes. This tendency, in the real space, is expressed as a formation of larger structures. In the real space, the same tendency is expressed by increasing the size of the leading bubbles and swapping the smaller bubbles downstream the interface. These two representations were demonstrated both experimentally and numerically. The real space concept led Alon et al. [11] to construct a statistical model that predicts the asymptotic structure of the interface. In their study, a rate equation, which counts the bubbles that were swapped away and the creation of a new bigger bubble in the interface, was presented. After numerically solving that equation, a self-similar behavior was observed.

Under the re-shock conditions, the problem is much more complex. In this scenario, the interface experiences another strong but short acceleration pulse. The interface is in its nonlinear stage, namely, $a/\lambda > 0.1$ when the acceleration pulse acts. In this section, we will present an experimental study that is focused on the initial stages of the interface after it experiences a re-shock. By utilizing the advantages of the planar Mie scattering visualization (PMSV) in a shock tube, we succeeded in monitoring the violent interaction of the second shock wave with the interface in a multi-bubble interface configuration.

2.2 Experimental Apparatus

The experiments were conducted in a vertical shock tube apparatuses. The driver and driven sections were 1.95 and 3.75 m long, respectively. The shock tube cross section was 80 × 80 mm, while the test section length was 580 mm. The interface was created between the air in the driven section that was mixed with cigarette smoke and SF_6 that was filled in the test section. A smooth contact surface was created between the driven and the test sections. This was achieved by continuously introducing smoked air and SF_6 into their two sections [12]. Exhausting these gases through two small horizontal slits at the two sidewalls of the shock tube generated a stagnation surface between the smoked air and the SF_6. In the above-described configuration, the re-shock hit the interface after about 5.5 ms, and there were about 3 ms more before the reflected expansion wave (from the driver's end-wall) interacted with the interface.

The PMSV system was implemented in the system where the Nd:YAG pulsed laser was used as a light source. A Phantom V12.1 high-speed camera that was synchronized with the laser pulses was used. The experimental setup is presented in Fig. 1a.

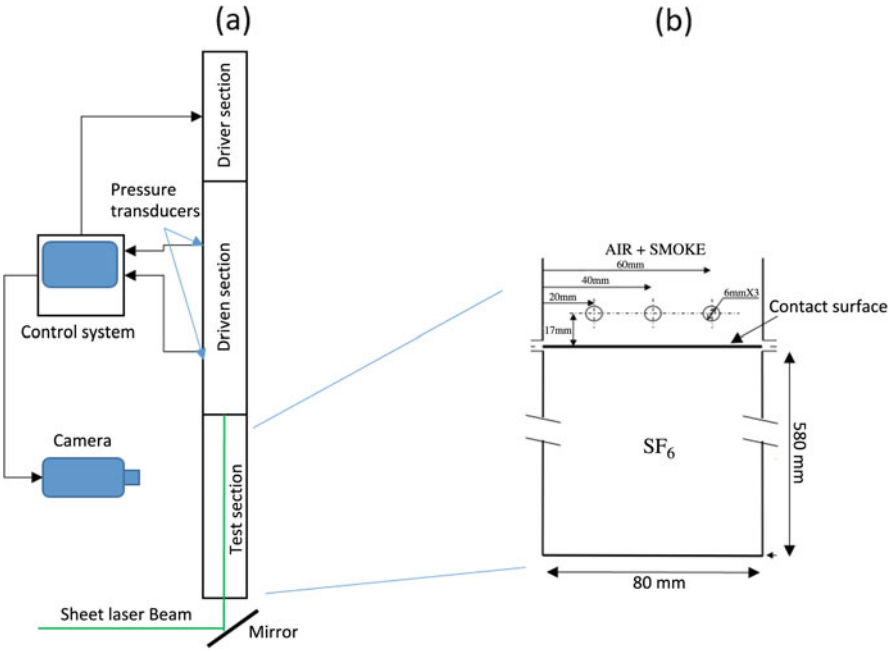

Fig. 1 (**a**) The vertical shock tube system. (**b**) The test section

In order to create an initial perturbation on the interface, we deformed the shock wave just before interacting with the interface. In this technique, a multi-bubble configuration was formed. The transmitted shock propagated in the SF_6 and became planar, reflected from the end-wall, and interacted with the perturbed interface again. The deformation of the shock was done by introducing obstacles above the interface. The obstacle configuration is presented in Fig. 1b. In this configuration, a 2D shock deformation that fits the needs of the experiments is created.

The deformed shock that crossed the planer contact surface generated a 2D multimode perturbation on it. In Fig. 2 this perturbation is presented at four different times. The perturbation growth is clearly seen. The vortices generated by the shock wave at the vicinity of the contact surface are the mechanism that governs the contact surface shape.

The optical system that was used included a cylindrical telescope to generate a sheet laser beam that entered the test section from a PMMA window that acted as the end-wall of the test section. The sidewalls of the test section were made of PMMA too in order to enable side visualization at any distance from the end-wall. The field of view of the camera was limited to 200 mm by 200 mm. Hence, in order to capture the entire interface evolution, the camera was moved to the required height.

The interface shape was measured using an in-house image-processing procedure. The contrast changes were found in each vertical pixel line, and the interface position point was found. By connecting all the points, the interface contour was constructed in each image frame.

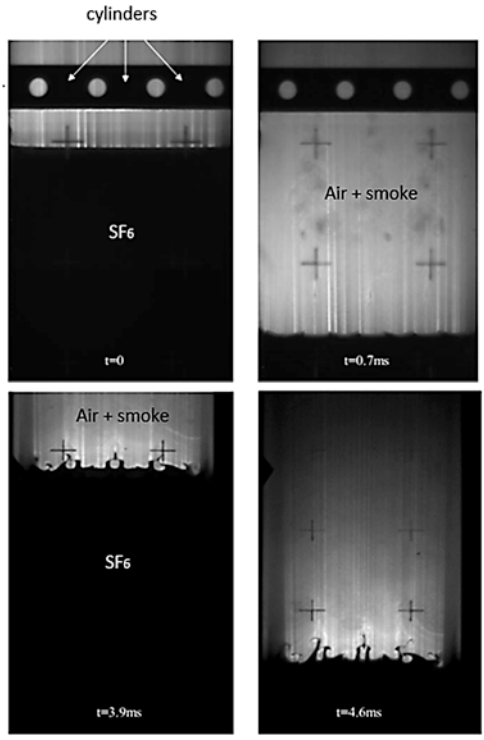

Fig. 2 Generation and evolution of the initial perturbation before the re-shock

2.3 Results and Discussion

After finding the position of the interface where the re-shock interacted with the interface, we adjusted the camera height to capture the interface evolution. A set of images from the experiment is presented in Fig. 3. The Mach number was 1.2. The reflected shock hit the perturb interface at $t = 0$.

The growth of the perturbation before the re-shock is saturated. Little change in the perturbation spectrum was observed. After the re-shock ($t > 0$), the interface experienced a dramatic deformation, and a notable nonlinear behavior was observed. The perturbation overall width was compared to numerical simulations (for more details about the numerical code, see [13]). A comparison between three different experiments and the simulation results is presented in Fig. 4. The initial conditions for the simulation were the measured initial perturbations in the experiments.

By taking advantage of the Mie scattering images, we could monitor the small details developing on the interface. As the first notable feature, we note that there is a phase inversion to the large-scale objects on the interface. The phase inversion is presented in Fig. 5a. This phase inversion occurred in the case of heavy to light configuration (the re-shock travel from FS_6 to air). Three bubbles before the re-shock invert to three spikes after the re-shock. Furthermore, the small-scale features experience merging process as demonstrated in Fig. 5b.

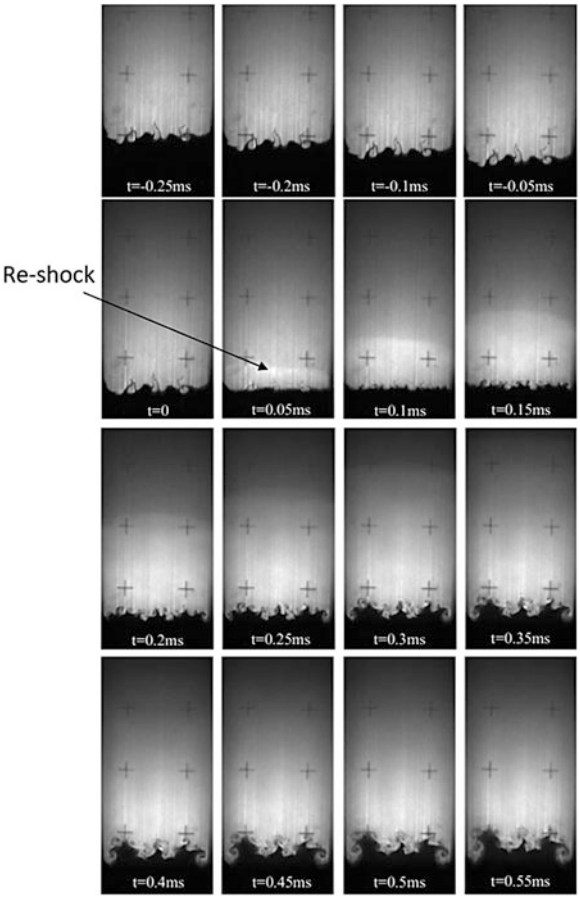

Fig. 3 A set of images from the air/SF_6 experiment with $M = 1.2$

We note that the merging process after the re-shock occurred faster than the prediction by the well-known theory. In Fig. 5b the wavelength and amplitude of two bubbles that experienced merging are almost the same. This means that the merging time of this two neighboring bubbles should take relatively long time as predicted by Hecht et al. [10]. This observation led us to distinguish between two different processes: (1) bubble competition and (2) bubble merging. Bubble competition is the process where a large bubble overtakes the space of a smaller bubble as demonstrated in Fig. 6a. Bubble merging process is the case where the spike between two neighboring bubbles is "closed" and the two bubbles become one bubble as demonstrated in Fig. 6b. The merging process occurred due to the increase of the bubble sideway to any two neighboring bubbles regardless of their size and therefore can be related to the evolution of a single bubble in the nonlinear stage. The competition process is related to the wavelength ratio of the two competing bubbles [10].

The same observation was found also in the numerical simulations.

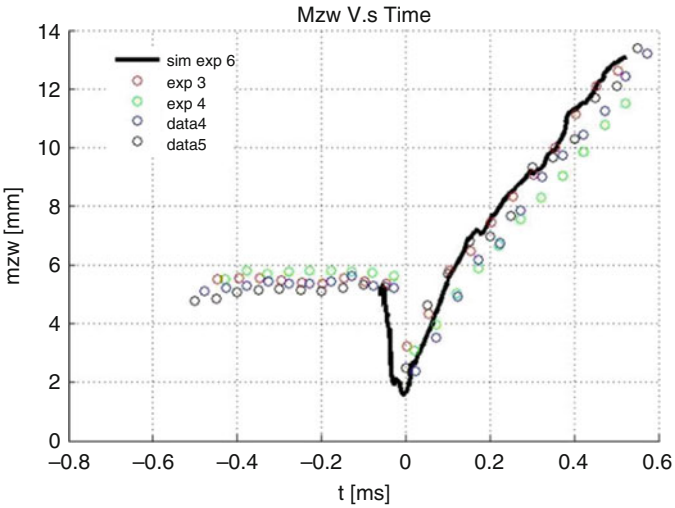

Fig. 4 Compression of the overall perturbation width between the experiments and the numerical simulation

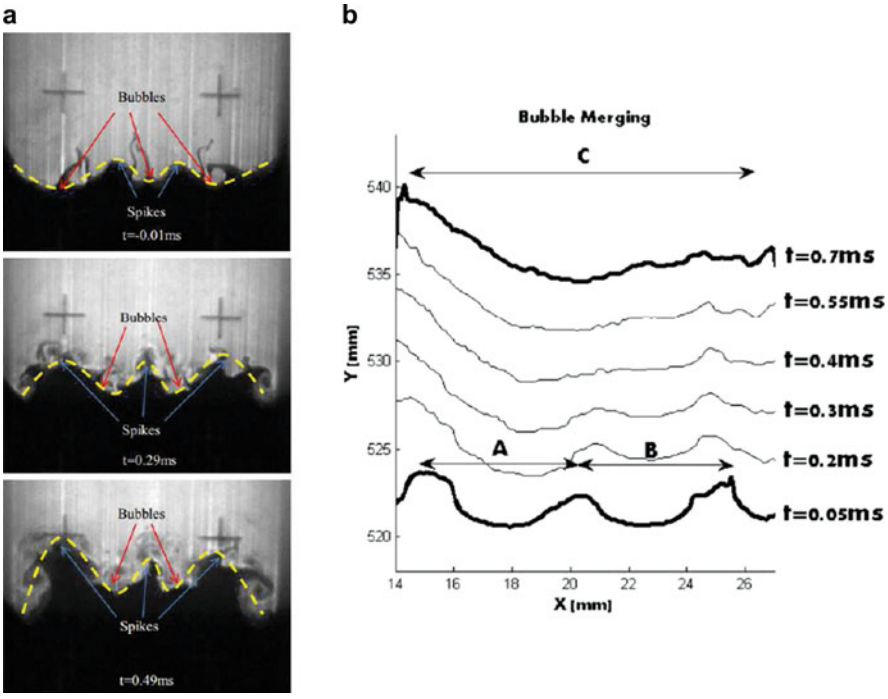

Fig. 5 (**a**) Contact surface phase inversion, (**b**) small-scale merging process

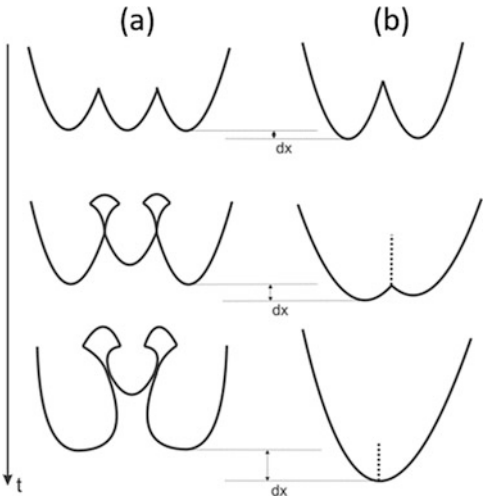

Fig. 6 (**a**) Bubble competition, (**b**) bubble merging

3 Starting Process in Converging-Diverging Nozzle

3.1 Introduction

The unsteady event occurring during the time after an incident shock propagates a nozzle and until a steady flow is achieved is called the "starting process." The starting process of supersonic planar nozzles has been the subject of a great amount of the shock tube research in the past. Initially this was motivated by the need to clearly separate the unsteady and quasi-steady parts of the expensing flow and thus specify the so-called "test time" period of shock tube tunnels. The most common and convenient technique to investigate the starting process is optical photography using schlieren, shadowgraph, or interferometry methods. Among the best-known images illustrating the starting process are those published by Amann [14]. It was clearly shown that the starting flow initiated by the primary shock (PS) wave included the contact surface (CS) and a secondary shock (SS). Smith [15] was the first to show that the unsteady expansion wave (UEW) which followed the SS could also affect the total duration of the starting flow. Actually, the SS initiated a flow separation at the nozzle sidewalls and transient structure of the separation points (SPs). The boundary layer separation was a natural process; it was the means by which a viscous flow adjusted to its surroundings under particular conditions. Next, the complex phenomenon that required fundamental knowledge on the parameters of the external flow and the condition inside the boundary layer was discussed by Dussauge and Piponniau [16]. Flow separation may also cause significant effects on the trajectory of the SS and increase the total duration of the starting flow pattern.

There is a renewed interest in nozzle starting phenomena due to wide application of transient nozzle flow in various devices. The effect of separation, for example, becomes important inside the nozzles of rockets, missiles, and/or supersonic

aircraft, where it is usually undesirable since it can cause a dangerous lateral force, which can damage the nozzle [17]. On the other hand, flow separation and the resulting instability of the exit plume could have a positive effect when used in high-speed mixing devices [18]. The past decade has seen a qualitative advancement of our understanding of the physical phenomena involved in flow separation in supersonic nozzles. In particular, the problem of side loads due to asymmetric pressure loads, which constitutes a major restraint in the design of nozzles for satellite launchers, become significant [19]. The development in this field is largely motivated by the demand for high-performance nozzles in rocket engineering. In the following, a short description of the experimental test section that was attached to the shock tube that was described in Sect. 2.2 is given.

3.2 The Experimental Apparatus

In order to control the asymmetry of the nozzle, we designed a symmetric 2D nozzle that one of its halves was attached to a linear translator that controlled the misalignment between the two half nozzles. The schematic design of the nozzle is presented in Fig. 7.

The distance Δ represents the asymmetry parameter where for the symmetric nozzle $\Delta = 0$. The other geometrical parameters are $R = 10 \pm 0.01$ mm; $L = 142.87 \pm 0.01$ mm; throat width $h_c = 9.5 \pm 0.01$ mm; and nozzle half angle $\alpha = 15 \pm 0.01°$. The range of the nozzle asymmetry parameter, Δ, was $0 < \Delta < 3.5$ mm. All the geometrical parameters but Δ were kept unchanged in all the experiments. The nozzle surface was very smooth. Each half of it was polished to a mirror roughness lever ($\varepsilon \sim 0.5\ \mu$m). Two Mach numbers were used, $M = 1.68$ and $M = 1.86$. The main diagnostic system was based on schlieren flow visualization by

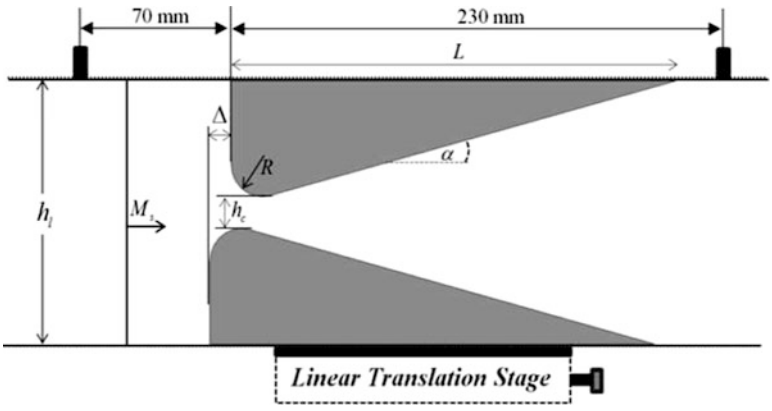

Fig. 7 Schematic illustration of the nozzle used

high-speed photography. The light source for the schlieren system was the doubled-frequency Nd:YAG pulsed laser (532 nm) at a rate of 20,000 pulses/s. A high-speed Phantom v12.1 digital camera synchronized with the laser was used. Measurements of the primary shock, secondary shock, and separation point locations visible in each image were obtained via an in-house Matlab®-based code.

3.3 Results and Discussion

Typical flow images of this series are shown in Fig. 8 for three different time instances after the incident shock impinging the nozzle front. At the arrival of the incident shock wave, both lateral parts of the incident shock wave are reflected at the parts of the nozzle entrance and propagate upstream as RS. The central part of the incident shock wave enters the nozzle throat and forms PS propagating into the quiescent gas occupying the nozzle. This generates the transverse flow to the main shocks that propagate toward the plane of symmetry where they collide and transmit with each other while forming a Mach configuration (MR). This configuration could be considered as a result of the RS reflections at an imaginary solid plane replacing the plane of symmetry. The MR finally generates two slip lines (SLs), which are clearly seen in Fig. 8b (a closer look at this SL reveals a Kelvin-Helmholtz instability that will be discussed later). The symmetry of the input flow pattern ensured the symmetry of the flow pattern inside the nozzle. A large difference in the tangential velocities at the CS separating the gases, which originally occupied the nozzle from the upstream flow, generated a series of small vortices that are also seen in Fig. 8b. The series of transverse shock waves behind the PS demonstrated repeated reflections between the nozzle walls. Soon a SS, which is facing upstream because of the pressure gradient created in the nozzle, appeared. However it was swept downstream by the flow expanding from the nozzle throat. Due to interactions with the boundary layers, the SS was bifurcated at the wall creating the flow separation. Two separation points (SPs) and the resulted bubbles of turbulent boundary layer fluid are clearly visible in Fig. 8b. The separation effect finally gave rise to two oblique shock waves, which move downstream and then intersect with each other. Interestingly, despite negligibly small asymmetry of the nozzle setup, the positions of the left, $(SP)_L$, and the right, $(SP)_R$, separation points in Fig. 8c do not coincide. A visible asymmetry in the final flow pattern led us to test this effect in more details.

In an asymmetric nozzle, the structure of the shock wave system is more complex. As the incident shock impinges the nozzle front, the left part of it (RS_L in Fig. 9) is reflected and propagates upstream, while the right part of the incident shock just reaches the nozzle front. A simple regular reflection (RR) can be seen on the nozzle left side. This RR changes to a Mach reflection (MR) on both sides of the nozzle (blue arrows in Fig. 9b). The two triple points travel toward the center and later meet; this motion generates a distinct jet at the interaction point of the two triple points (see Fig. 9c).

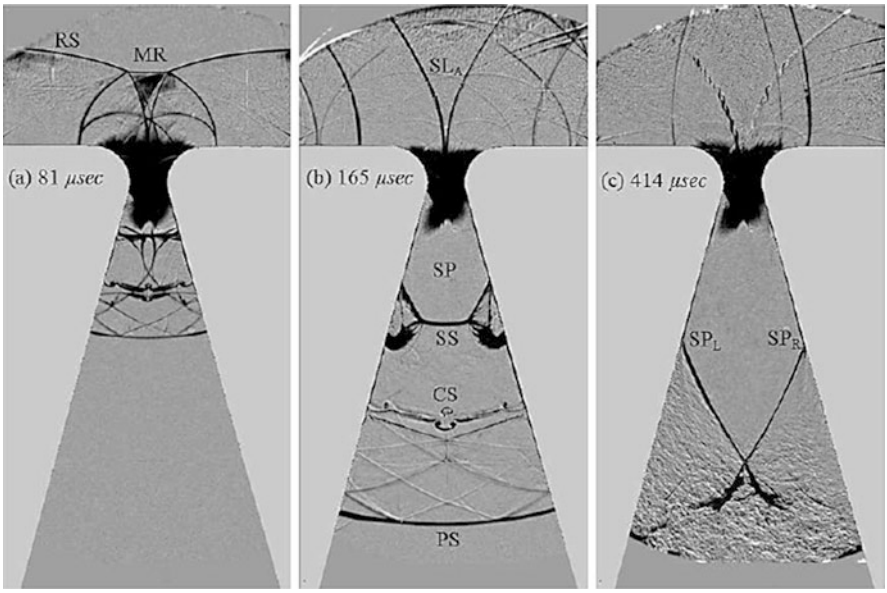

Fig. 8 Schlieren images of the starting flow, $M_s = 1.86$, $R = 10\ mm$, $\Delta = 0.05$

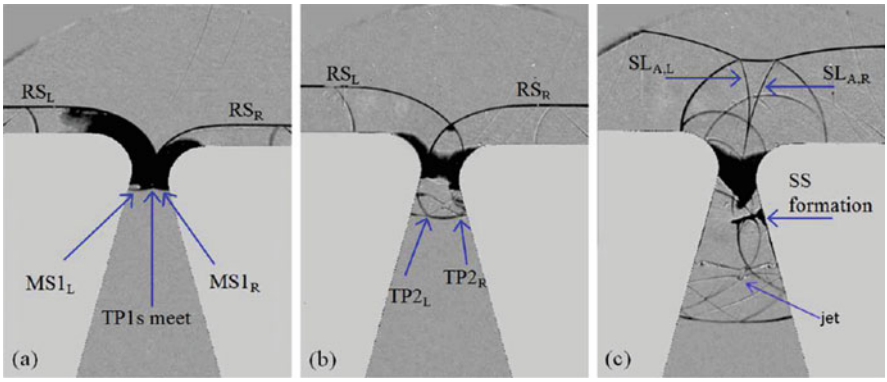

Fig. 9 Schlieren images of the starting process in an asymmetric nozzle, $M_s = 1.86$ and $\Delta = 3.17$ mm. (**a**) The RR that was formed after the incident shock hit the nozzle front transformed into an MR on both sides. The left Mach stem $MS1_L$ is longer than the right Mach stem $MS1_R$. Both TPs meet closer to the right side of the nozzle; (**b**, **c**) $M_s = 1.68$, $\Delta = 3.12$ mm; (**b**) shows a new TP2 (right and left) traveling toward the wall in an asymmetric manner. They were formed after the regular reflection of MS1 turned into an MR. The formation of the SS near the right side of the nozzle is clear in frame (**c**)

One can see that the location of this meeting point is closer to the right wall of the nozzle. The RR of MS1 turns into an MR, and a new TP2 (right and left) travels toward the wall in an asymmetric manner (Fig. 9b) before vanishing and ejecting its SL.

The SS formation near the right side of the nozzle is visible at 86 μs (see Fig. 9c). This is in contrast to the symmetric case where the SS formation occurs simultaneously from both sides of the nozzle. It is obvious from the images that even before the SS fully occupies the whole cross section, its right part interacts with the boundary layer and a lambda configuration appears. A closer look at the SS left side reveals that there is a connection to the PS via the complex shape of shock waves and SLs.

In each frame the separation points (SP – left and right) were measured, and there, trajectories and height differences were plotted. In Fig. 10a–c the left, the right, and the height differences are presented.

From the study, the following salient points of practical interest can be summarized. It was found that flow asymmetry appears even when the shifting parameter is small (typical accuracy of the nozzle setup is about 0.05 mm). Four stages of the asymmetric flow pattern were found showing that the relative position of the two SPs is first inverted and then stabilized. A fundamental difference between small and large shifting of the half nozzle was found. For small shifting, the fourth stage of the asymmetric flow pattern, where the relative positions of the two SPs were inverted, repeated itself. Consequently the relative positions of the SPs transversed several times. This was in contrast to the case of large shifting of the half nozzle where the relative positions of the SPs transversed only once. The arrival of the reflected shock PS_{ref} (that appeared as a result of the PS reflection at the nozzle exit) at the separation zone inside the nozzle caused a sudden change in the shock structure. The separation point trajectories lost stability, and an asymmetric flow pattern was established. At a later stage of the starting process, after the PS_{ref} arrived at the separation zone, the whole separation configuration oscillated upstream and then downstream in a wavy manner. Unlike the small shifting case where the SP trajectory continued in an approximately symmetric manner, in the large shifting case, the SP trajectories diverged, and a significant asymmetry pattern was formed.

4 Summary

In the presented studies, we focused on two different subjects: the shock-induced hydrodynamic instability developed on the contact surface between two fluids and the starting process in a 2D nozzle. In the first study, we found that the complex case of multimode perturbation, after the re-shock merging process occurred, was much faster than the well-known bubble competition process. In the nozzle study, we noted that there was a difference between significant asymmetry and minor asymmetry cases in terms of the overall nozzle flow patterns. Moreover, even at a very small geometrical asymmetry (0.05 mm), the flow became asymmetric as

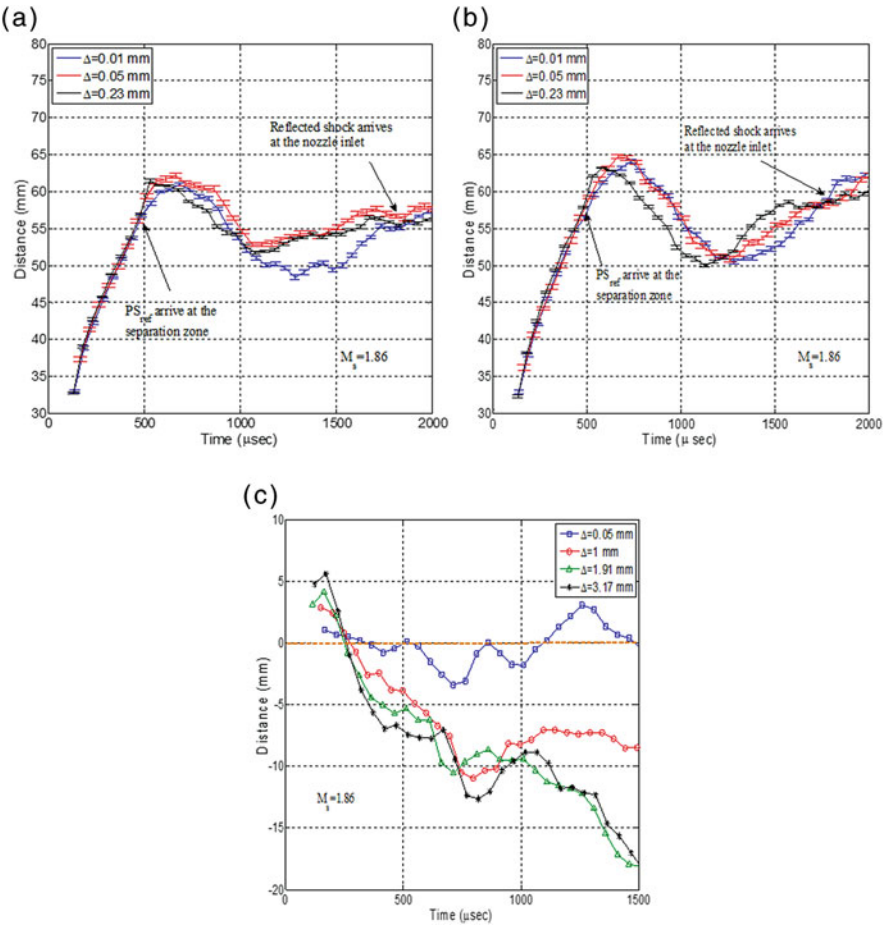

Fig. 10 (**a**) Left (upstream half nozzle side) SP trajectory for $M_s = 1.86$ and small nozzle shifting $0 < \Delta < 0.23$ mm. (**b**) Right (downstream half nozzle side) SP trajectory for $M_s = 1.86$ and small nozzle shifting $0 < \Delta < 0.23$ mm. (**c**) SP trajectory differences for $M_s = 1.86$ for four different shifting parameters $0 < \Delta < 3.5$ mm

well. This led to the conclusion that there is a critical equilibrium of the flow in the nozzle and any small disturbance led to major asymmetry flow patterns.

References

1. P.M. Rightley, P. Vorobieff, R. Martin, R.F. Benjamin, Evolution of a shock-accelerated thin fluid layer. Phys. Fluids **9**(6), 1770–1782 (1997)
2. G.I. Taylor, The instability of liquid surfaces when accelerated in a direction perpendicular to their planes. Proc. Roy. Soc. **A201**, 192–196 (1950)

3. R.D. Richtmyer, Taylor instability in shock acceleration of compressible fluids. Commun. Pure Appl. Math. **13**, 297–319 (1960)
4. E.E. Meshkov, Instability of the interface of two gases accelerated by a shock wave. Sov. Fluid Dyn. **4**, 101–108 (1969)
5. J.D. Lindl, R.L. McCrory, E.M. Campball, Progress toward ignition and burn propagation in inertial confinement fusion. Phys. Today **45**(9), 32–50 (1992)
6. D. Arnett, The role of mixing in astrophysics. Astrophys. J. Suppl. Ser. **127**, 2 (2000)
7. U. Alon, J. Hecht, D. Ofer, D. Shvarts, Power laws and similarity of Rayleigh-Taylor and Richtmyer-Meshkov mixing fronts at all density ratios. Phys. Rev. Lett. **74**(4), 534–537 (1995)
8. D. Ofer, D. Shvarts, Z. Zinamon, S.A. Orszag, Mode coupling in nonlinear Rayleigh-Taylor instability. Phys. Fluids B **4**(11), 3549–3561 (1992)
9. D. Layzer, On the instability of superposed fluids in a gravitational field. Astrophys. J. **122**, 1–12 (1955)
10. J. Hecht, U. Alon, D. Shvarts, Potential flow models of Rayleigh-Taylor and Richtmyer-Meshkov bubble fronts. Phys. Fluids **6**(12), 4019–4030 (1994)
11. U. Alon, J. Hecht, D. Mukamel, D. Shvarts, Scale invariant mixing rates of hydrodynamically unstable interfaces. Phys. Rev. Lett. **72**(18), 2867–2870 (1994)
12. M.A. Jones, J.W. Jacobs, A membraneless experiment for the study of Richtmyer-Meshkov instability of a shock-accelerated gas interface. Phys. Fluids **9**(10), 3078–3084 (1997)
13. N. Freed, D. Ofer, D. Shvarts, S.A. Orszag, 2-phase flow-analysis of self-similar turbulent mixing by Rayleigh-Taylor instability. Phys. Fluids A **3**, 912 (1991)
14. H. Amann, Experimental study of the starting process in a reflection nozzle. Phys. Fluids Suppl. **12**, 150–153 (1969)
15. C. Smith, The starting process in a hypersonic nozzle. J. Fluid Mech. **24**, 624–640 (1966)
16. J. Dussauge, S. Piponniau, Shock/boundary layer interactions: possible source of unsteadiness. J. Fluids Struct. **24**, 1166–1175 (2008)
17. A. Hadjadj, M. Onofri, Nozzle flow separation. Shock Waves **19**, 163–169 (2009)
18. A.D. Johnson, D. Papamoschou, Instability of shock-induced nozzle flow separation. Phys. Fluids **22**, 016102-1-13 (2010)
19. J. Ostlund, Supersonic flow separation. Appl. Mech. Rev. **58**, 143–177 (2005)